Bull. Spec. Astrophys. Obs., 2002, 54, 66–73

Some features of variation of the Hα line profile in the spectrum of α CYG. I. The spectra for the period July-September, 1998

A.Kh. Rzayev[a b]

[a] Special Astrophysical Observatory of the Russian AS, Nizhnij Arkhyz 369167, Russia
[b] Shamakhy Astrophysical Observatory of the Azerbaijan National AS, Yu. Mamedaliyev, Shamakhy

Received October 15, 2002; accepted October 20, 2002.

Abstract. A method is presented for a detailed study of time variation of radial velocity of the absorption Hα line in the α Cyg supergiant spectrum. The method allows us to study time variation of the radial velocity of the absorption line, blue and red halves of its contour and to determine the share of the contribution of these halves to the absorption radial velocity variation on different levels of the residual intensity. It was established that the absorption component may be divided into four levels. Time variation of the radial velocity of the absorption, blue and red halves of its contour, values of gradient (slope) of the radial velocity for these halves, and also the widths of the absorption component differ for different levels of residual intensity. The amplitudes of these variations also differ for different levels that testifies to stratification of radial velocities in the upper layers of the atmosphere where the stellar wind forms. 4 versions of radial velocity variability of the absorption component are determined which are caused by changes of velocity fields in the atmosphere of the star. At different moments of observations additional emission and absorption components of envelope origin due to matter outflow from the star surface are superimposed on them.

Key words: stars: supergiants — stars: spectrum — individual: α Cyg

1. Introduction

The supergiant α Cyg is one of the bright stars on the northern sky, and for this reason it is the object of many observations from the far UV to the radio range (Aufdenberg et al., 2002). It has been established that the variability of radial velocities of ion lines in the spectrum of α Cyg is caused by the motions of pulsation type which occur in its atmosphere (Lucy, 1976). In supergiants of spectral class A, Hα is the only windsensitive line in the optical range. A detailed study of time variations of the Hα profile can help us reveal the relationship between the atmosphere pulsation and stellar wind.

The supergiant α Cyg was studied in detail by the "Heidelberg" group (Kaufer et al., 1996a, 1997) on the basis of long continuous spectral observations with high (R=20000) resolution. With the help of dynamical spectra they discovered that the Hα profile is variable. Variability in Hα is found to be quite symmetric about the systemic velocity and is mainly due to variable blue and red-shifted emission superimposed on almost constant photospheric and/or wind profiles (furtehr we will call it as "basic" absorption profile). It is noted that because of the complex character of Hα profile variability, it is very difficult to determine the characteristic time of these variations. The characteristic time of the Hα equivalent width variation is close to the period of rotation of the star.

In our opinion, a more optimum method for a detailed study of the complex variable structure of the Hα profile is the measurement of the radial velocity of the absorption at different levels of residual intensity. Since the Hα absorption forms throughout the entire atmosphere height the study of time variations of some parameters of the line at different levels of residual intensity will give information about the velocity field and its variations with depth in the atmosphere. In the present paper such an investigation is carried out for the Hα line of the supergiant α Cyg.

2. Spectral data and techniques of measurements

During two months in 1998, from 24.07 to 21.09, 40 CCD spectra of the supergiant α Cyg A2 Ia were obtained at the Shamakhy Astrophysical Observatory

with a resolution of R=36000 and a S/N ratio of $150 \leq S/N \leq 500$. The echelle spectrograph CEGS with a CCD of 530 × 580 was used. The spectrometer itself, the methods of obtaining, processing and reduction of the spectra were described in the papers by Musaev (1993) and Rzayev et al. (1999a). The processing of echelle spectra was carried out in the standard procedure with the aid of the programme package DECH20 (Galazutdinov, 1992). The photometric and position precision of line measurements was reported in the papers by Chentsov (1995) and Rzayev et al. (1999a,b). Systematic errors of the radial velocity measurements were checked with the help of the telluric lines of H_2O and O_2. The root-mean-square deviation from the mean found from 60 telluric lines is -0.2 ± 0.6 km/s (Rzayev et al., 1999b).

During the first two nights two spectra of the star were obtained on each night, on the rest of the nights four spectra were obtained on each night. No rapid variations during the night were found. That is why, the profiles obtained on one night or subsequent nights, but showing no variations, were summed up and averaged. The examples of the Hα line profiles thus obtained (normalized to the continuum) are presented in Fig. 1. The blue and red wings get continuum at about ±520 km/s. The continuum level is shown with horizontal lines. In Fig. 1 the red wing emission of the Hα line for each date is corrected for the telluric lines λ6563.5, 6564.0 and 6564.2 Å. The scale on the r_λ axis is the same for all the profiles and is indicated in the lower right part of the figure. At the last stage of the observations no significant variations of the radial velocities of the Hα line and its individual details were revealed within the measurement errors. To show how separate absorption details change during these four nights, the profiles obtained on the first (18.09 + 19.09) and on the last (20.09 + 21.09) two nights are presented in Fig. 1 as F_1 and F_2, respectively.

In Table 1 are given the following data: N is the number of spectrograms obtained on the indicated dates; S/N is the signal-to-noise ratio in the net spectrum; r_0 is the residual intensity at the line centre for the emission (Em.) and absorption (Abs.) components; V_r is the radial velocity of individual absorption components or the details indicated in Fig. 1. All these details are clearly seen on both the individual spectra derived on one night and the spectrum obtained as a result of their summation. The measurements were made on both the individual and the summary spectra. For the blue part of the absorption the radial velocity measurement error at the level $r_\lambda = 1.0$ is mainly caused by the uncertainty of plotting the line contour and is ±10 km/s, while for the value $0.96 \leq r_\lambda < 1.0$ and $r_0 \leq r_\lambda \leq 0.95$ it is not larger than ±2.0 and ±0.5 km/s, respectively.

In the programme package DECH20 there are two modes of measuring the radial velocity of lines (Galazutdinov, 1992). The first one is the "Determination of the radial velocity from the line profile". After definition of the line boundaries a mirror image of the line profile appears. By means of overlapping the direct and mirror images the radial velocity is found. For asymmetric lines, through matching of the two images at different levels of the profile, one can determine the radial velocity of the bisector for different regions (for instance, for the core of the central part and the wing) of the line. The second mode is the "Determination of the radial velocity by points". By means of pointing an indicator to any point of the line contour and having specified the laboratory wavelength of this line, it is possible to measure the radial velocity at this point. For measuring the radial velocity of symmetric absorption lines the first mode is faster and more convenient. To measure the radial velocity of the bisectors of asymmetric lines, the second mode is optimum.

To reveal the variability of the absorption component and to study the differential shifts of its individual parts, we applied the following method. The radial velocity of the absorption was measured at different levels of its intensity with a step $\Delta r_\lambda = 0.01 \div 0.005$ in the interval $(r_0 + 0.02) \leq r_\lambda \leq 1.0$. For each value of r_λ the radial velocities of the blue and red halves of the absorption contour were measured. The arithmetic mean of these values yields the radial velocity of the absorption bisector. The radial velocities thus derived for different levels of r_λ are presented in Table 2. For short and for the best comparison we present the results of measurement for the absorption line and blue and red halves of its contour in one table. In each square of Table 2 in the upper line (left and right parts, respectively) the radial velocities for the blue (V_b) and red (V_r) halves of the absorption contour are presented, while in the lower middle part is given the radial velocity of the absorption (V_r), where $V_r = (V_b + V_r)/2$. The measurement of the radial velocity by this method allowed us to determine the values of the radial velocity gradient for the blue and red halves of the absorption contour at different levels of residual intensity. We determined the slope as the ratio $\Delta V_r/\Delta r$ and computed it for both halves of the absorption contour from the line core to the wing with a step of $\Delta r = 0.05$. On some dates (for instance, Fig. 1, F_1, F_2) when the discrete absorption components observed on the blue half of the contour presented a severe problem in the determination of the radial velocity gradient, the profiles plotted by a gaussian or manually were used.

3. Results of measurements

The investigations have shown that by the value of the radial velocity gradient and its time variation the

Table 1: *Some parameters of the* Hα *line of the supergiant α Cyg. For designation see the text*

Date	N	S/N	r_0		V_r, km/s								
			Em.	Abs.	K_1	K_2	K_3	K_4	K_5	K_6	K_7	K_8	K_9
24.07.98	2	150	1.045 ±0.006	0.526 ±0.004	-28.0 ±1.2	-	-		-	-	-	-	-
29.07.98	2	150	1.070 ±0.007	0.533 ±0.008	-27.0 ±1.0	-	-		-	-	-	-	-
10.08.98	4	200	1.090 ±0.005	0.539 ±0.006	-26.4 ±0.8	-37.0 ±0.4	-		-	-	-	-	-
(27+28). 08.98	8	300	1.108 ±0.008	0.556 ±0.004	-25.0 ±1.2	-	-	-50.0 ±0.6	-	-	-102.2 ±0.5	-	-
(31+01). 08/09.98	8	300	1.074 ±0.003	0.570 ±0/004	-25.3 ±1.2	-	-		-76.0 ±0.3	-	-	-	-
18+19+20 +21).09.98	16	400	1.098 ±0.002	0.634 ±0.01	-26.3 ±0.5	-	-45.0 ±0.4		-	-83.5 ±1.5	-	-111.5 ±0.6	-151.0 ±3.2

Table 2: *Heliocentric radial velocities of the* Hα *line absorption and blue and red halves of its absorption contour at different levels of the residual intensity. For designations see the text*

r_λ	V_r km/s					
	24.07.98	29.07.98	10.08.98	(27+28).08.98	(31.08+01.09).98	(18+19+20+21).09.98
	A	B	C	D	E	F
I						
1.000	-520.0 38.0 -241.0	-520.0 38.0 -241.0	-520.0 29.0 -245.5	-520.0 33.0 -243.5	-520.0 38.0 -241.0	-520.0 26.0 -247.0
0.990	-400.0 37.0 -181.5	-400.0 37.0 -181.5	-400.0 28.0 -186.0	-400.0 2.0 -184.0	-400.0 37.0 -181.5	-400.0 25.0 -187.5
0.980	-290.0 36.0 -127.0	-290.0 36.0 -127.0	-290.0 27.0 -131.5	-290.0 31.0 -129.5	-290.0 36.0 -127.0	-290.0 24.0 -133.0
0.970	-230.0 35.0 -97.5	-230.0 35.0 -97.5	-230.0 26.0 -102.0	-230.0 30.0 -100.0	-230.0 35.0 -97.5	-230.0 23.0 -103.5
0.960	-200.0 34.0 -83.0	-200.0 34.0 -83.0	-200.0 25.0 -87.5	-200.0 29.0 -85.5	-200.0 34.0 -83.0	-200.0 22.0 -89.0
II						
0.930	-131.0 31.0 -50.0	-131.0 31.0 -50.0	-142.0 22.0 -60.0	-158.0 26.0 -66.0	-158.0 31.0 -63.5	-174.0 19.0 -77.5
0.920	-126.0 30.0 -48.0	-126.0 30.0 -48.0	-137.0 21.0 -58.0	-153.0 25.0 -64.0	-153.0 30.0 -61.5	-169.0 18.0 -75.5
0.910	-121.0 29.0 -46.0	-121.0 29.0 -46.0	-132.0 20.0 -56.0	-148.0 24.0 -62.0	-148.0 29.0 -59.5	-164.0 17.0 -73.5
0.900	-116.0 28.0 -44.0	-116.0 28.0 -44.0	-127.0 19.0 -54.0	-143.0 23.0 -60.0	-143.0 28.0 -57.5	-159.0 16.0 -71.5
III						
0.850	-104.0 23.0 -40.5	-104.0 23.0 -40.5	-115.0 14.0 -50.5	-126.0 18.0 -54.0	-131.0 22.0 -54.5	-141.0 11.0 -65.0
0.800	-95.0 18.0 -38.5	-95.0 18.0 -38.5	-106.0 9.0 -48.5	-114.0 13.0 -50.5	-119.0 16.0 -51.5	-119.0 6.0 -56.5
0.750	-86.0 13.0 -36.5	-86.0 13.0 -36.5	-97.0 4.0 -46.5	-105.0 8.0 -48.5	-110.0 10.0 -50.0	-97.0 1.0 -48.0
0.700	-77.0 8.0 -34.5	-77.0 8.0 -34.5	-88.0 1.0 -44.5	-96.0 3.0 -46.5	-101.0 4.0 -48.5	-58.0 -6.0 -32.0
IV						
0.650	-68.0 3.0 -32.5	-68.0 3.0 -32.5	-79.0 -6.0 -42.5	-87.0 -3.0 -45.0	-92.0 -4.0 -48.0	-36.0 -16.0 -26.0
0.600	-62.0 -2.0 -32.0	-49.0 -8.0 -28.5	-62.0 -14.0 -38.0	-78.0 -13.0 -45.5	-83.0 -14.0 -48.5	-
0.550	-45.0 -15.0 -30.0	-37.0 -23.0 -30.0	-43.0 -24.0 -33.5	-	-	-

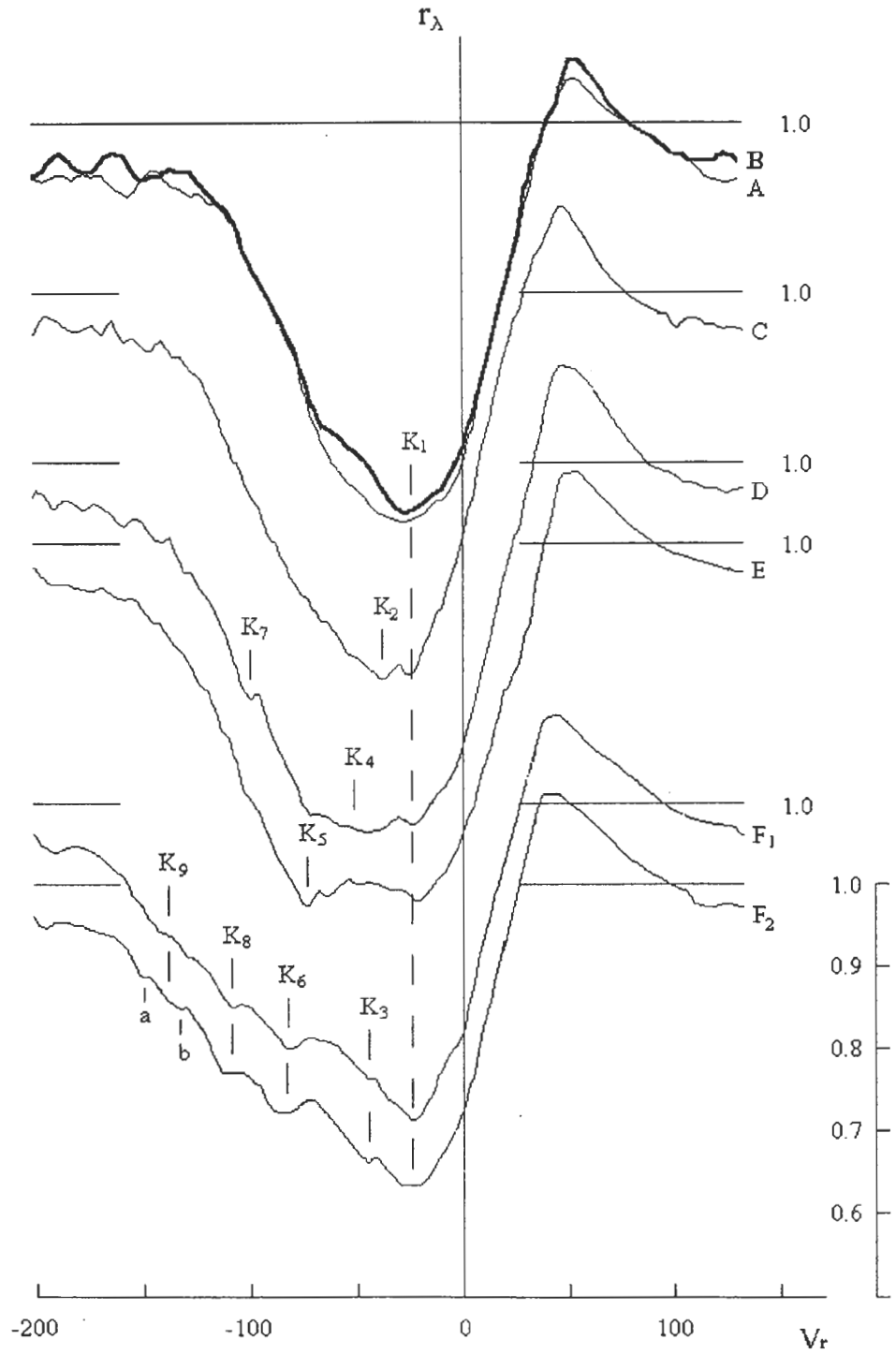

Figure 1: *Hα line profiles in the spectrum of the supergiant α Cyg. For designations see the text.*

absorption Hα can be tentatively divided into four levels which are shown by the bold horizontal lines in Tables 2, 3 and 4: level I is the wing, where $0.96 \leq r_\lambda \leq 1.0$, and transition part, where $0.93 \leq r_\lambda \leq 0.96$; level II is the upper part, where $0.9 \leq r_\lambda \leq 0.93$; level III is the middle, where $0.7 \leq r_\lambda \leq 0.85$; level IV is the core, where $r_0 \leq r_\lambda \leq 0.7$.

The time variation of the radial velocity of the absorption, blue and red halves of its contour, the radial velocity gradient values for these halves and also the absorption widths are different for these levels.

The values of time variations of the radial velocity

Table 3: *Time variations of the radial velocity of the* Hα *line absorption, blue and red halves of its contour at different levels of the residual intensity. For designations see the text*

	ΔV_r, km/s				
r_λ	B-A	C-B	D-C	E-D	F-E
I					
1.000	0.0 0.0	0.0 -9.0	0.0 4.0	0.0 5.0	0.0 -12.0
	0.0	-4.5	2.0	2.5	-6.0
0.990	0.0 0.0	0.0 -9.0	0.0 4.0	0.0 5.0	0.0 -12.0
	0.0	-4.5	2.0	2.5	-6.0
0.980	0.0 0.0	0.0 -9.0	0.0 4.0	0.0 5.0	0.0 -12.0
	0.0	-4.5	2.0	2.5	-6.0
0.970	0.0 0.0	0.0 -9.0	0.0 4.0	0.0 5.0	0.0 -12.0
	0.0	-4.5	2.0	2.5	-6.0
0.960	0.0 0.0	0.0 -9.0	0.0 4.0	0.0 5.0	0.0 -12.0
	0.0	-4.5	2.0	2.5	-6.0
II					
0.930	0.0 0.0	-11.0 -9.0	-16.0 4.0	0.0 5.0	-16.0 -12.0
	0.0	-10.0	-6.0	2.5	-14.0
0.920	0.0 0.0	-11.0 -9.0	-16.0 4.0	0.0 5.0	-16.0 -12.0
	0.0	-10.0	-6.0	2.5	-14.0
0.910	0.0 0.0	-11.0 -9.0	-16.0 4.0	0.0 5.0	-16.0 -12.0
	0.0	-10.0	-6.0	2.5	-14.0
0.900	0.0 0.0	-11.0 -9.0	-16.0 4.0	0.0 5.0	-16.0 -12.0
	0.0	-10.0	-6.0	2.5	-14.0
III					
0.850	0.0 0.0	-11.0 -9.0	-11.0 4.0	-5.0 4.0	-10.0 -11.0
	0.0	-10.0	-3.5	-0.5	-10.5
0.800	0.0 0.0	-11.0 -9.0	-8.0 4.0	-5.0 3.0	0.0 -10.0
	0.0	-10.0	-2.0	-1.0	-5.0
0.750	0.0 0.0	-11.0 -9.0	-8.0 4.0	-5.0 2.0	13.0 -9.0
	0.0	-10.0	-2.0	-1.5	2.0
0.700	0.0 0.0	-11.0 -9.0	-8.0 4.0	-5.0 1.0	43.0 -10.0
	0.0	-10.0	-2.0	-2.0	16.5
IV					
0.650	0.0 0.0	-11.0 -9.0	-8.0 3.0	-5.0 -1.0	56.0 -12.0
	0.0	-10.0	-2.5	-3.0	22.0
0.600	13.0 -6.0	-13.0 -6.0	-16.0 1.0	-5.0 -1.0	-
	3.5	-9.0	-5.5	-3.0	
0.550	8.0 -8.0	-6.0 -1.0	-	-	-
	0.0	-3.5			

of the absorption and also of the blue and red halves of its contour at different levels of residual intensity are presented in Table 3 in the lower and upper left and right parts of each square, respectively. The value of the absorption width variation (full width of $\Delta\lambda$ in Å) is given in Table 4.

The study of time variability of the absorption has shown that two characteristic cases of variability can be isolated. The first one is due to the differential shifts of the blue and red halves of the absorption contour. The second one is caused by superposition of absorption and/or emission components of shell origin. In the second version of level III in the majority of moments of observations one can "neglect" (by means of plotting the contour manually) the effects of these components and to study the variability of the "purely" absorption profile.

The method we used for measuring the radial velocities allows us to estimate the share of contribution of the blue and red halves of the contour to the absorption radial velocity variation. The results obtained show that the amplitudes of the radial velocity variation of the absorption, blue and red halves of its contour also differ for the levels indicated above.

For the red half of the absorption contour in most observations the radial velocity gradient at levels I, II,

III, and IV is 5 km/s for every $\Delta r_\lambda = 0.05$, while the radial velocity variation amplitude (from the maximum extreme values of the radial velocity) is equal to all levels, about 12 km/s.

At level I the radial velocity of the blue half of the absorption contour is not time-variable within the measurement errors. The shifts of the absorption take place because of the radial velocity variations of the red half of its contour. The amplitude of the radial velocity variations of the absorption is 6 km/s.

At level II the radial velocity of the blue half of the absorption contour is time-variable and the amplitude of these variations is 44 km/s. Therefore the amplitude of the absorption radial velocity variations is 28 km/s. The value of the radial velocity gradient for the blue half of the absorption contour is not time-variable and for every $\Delta r_\lambda = 0.05$ it is -25 km/s.

At level III both the radial velocity gradient value and the radial velocity for the blue half of the absorption contour vary with time. The amplitude of the radial velocity variation is 18 km/s, 24 km/s and 12 km/s for the absorption and its blue and red halves, respectively. The radial velocity gradient value at the beginning of observations (24.07.98) is -9.0 km/s for every $\Delta r_\lambda = 0.05$. This value is likely to preserve for about 40 days, up to 01.09.98. Next, after 17 days, from 18.09.98 to 21.09.98 it becomes -22.0 km/s, which points to the fact that the velocity of expansion in the upper layers of the atmosphere increases (Table 2).

At level IV the absorption core is the most variable part of the Hα profile. Its variability is chiefly caused by the processes occurring in the star envelope, which have an effect both on the steepness of its blue and red halves and on their differential shift.

Time variation of the absorption width and its amplitude also differ for the above mentioned levels. On some nights at different levels different behaviour of variation is observed, i.e. within one level the absorption width increases, at the same time within another level it decreases (Table 4 (F–E)). The maximum amplitude of these variations is recorded in the absorption core at $r_\lambda = 0.65$ and makes $\delta(\Delta\lambda) \approx 1.5$ Å. This is probably caused by additional widening and/or narrowing of the contour because of the superposition of absorption and/or emission components of shell origin on the absorption profile. At other levels, where the effect of the shell on the absorption contour is not very significant and the absorption width variation is basically associated with the velocity field variation in the atmosphere of the star, the amplitude is 0.3, 0.7 and 0.5 Å for levels I, II, and III, respectively.

Table 4: *Time variations of the* Hα *line absorption width at different levels of residual intensity. For designations see the text*

r_λ	$\delta(\Delta\lambda)$,Å				
	B-A	C-B	D-C	E-D	F-E
I					
1.000	0.0	-0.197	0.087	0.109	-0.263
0.990	0.0	-0.197	0.087	0.109	-0.263
0.980	0.0	-0.197	0.087	0.109	-0.263
0.970	0.0	-0.197	0.087	0.109	-0.263
0.960	0.0	-0.197	0.087	0.109	-0.263
II					
0.930	0.0	0.044	0.438	0.109	0.088
0.920	0.0	0.044	0.438	0.109	0.088
0.910	0.0	0.044	0.438	0.109	0.088
0.900	0.0	0.044	0.438	0.109	0.088
III					
0.850	0.0	0.044	0.328	0.197	-0.022
0.800	0.0	0.044	0.262	0.175	-0.219
0.750	0.0	0.044	0.262	0.153	-0.481
0.700	0.0	0.044	0.262	0.131	-1.159
IV					
0.650	0.0	0.044	0.241	0.088	-1.488
0.600	-0.416	0.153	0.372	0.088	-
0.550	-0.350	0.110	-	-	-

4. Discussion of the results

Based on the above-mentioned results and from the data of Table 3 one can highlight 5 versions of radial velocity variations and absorption variability.

The absorption radial velocity variation occurrs due to:

- the shift of the absorption on the whole. In this case the width and the gradient of the radial velocity of the blue and red halves of the absorption contour do not change, i.e. they show the same positive or negative shift;
- the differential shift of the blue (the red one does not change) half of the absorption contour. A characteristic example is the case where on 10.08.98, as compared to the previous date (29.07.98), the absorption on the whole shows a negative shift, -9 km/s. And because of the additional shift of the blue half of the absorption contour by -2 km/s its total shift is -10 km/s, Table 3 (C–B), absorption level II;
- the differential shift of the red (the blue one is unchanged) half of the absorption contour. A typical example is the case (E–D) in Table 3, level II;
- the differential shift of the both halves of the absorption contour. A typical example is the case (D–C), Table 3, level II;
- additional superpositions of the absorption and/or emission components of shell origin on the photospheric profile in the previous 4 cases.

At different moments of observations we recorded from one (Table 1 and Fig. 1 A and B) to five (Table 1, F and Fig. 1 F_1 and F_2) of absorption components or details. They can be divided into three groups: constant component with a mean velocity $K_1 = -26.3 \pm 0.9$ km/s, components with radial velocities $K_2 = -37.0, K_3 = -45.0, K_4 = -50.0$ km/s observed within $r_0 \leq r_\lambda < 0.7$, and the components K_6, K_7, K_8 and K_9 with velocities (in km/s) $-170.0 < V_r < -80.0$ observed within $0.7 \leq r_\lambda < 0.93$.

As can be seen from Fig. 1 (F_1 and F_2), at the final stage of observations during four nights, we observe the intensity of the components K_3, K_6 and K_8 to enhance. On these dates a faint component with a mean velocity $K_9 = -151.0 \pm 3.2$ km/s is observed. It is likely to be composed of two components $K_9(a) = -166.5 \pm 3.6$ km/s and $K_9(b) = -136.0 \pm 4.0$ km/s and during these days its intensity rises.

However, during these nights neither in the absorption itself, nor in its individual components, within the measurement errors, radial velocity variations are observed. Therefore, despite their high radial velocities, we believe that K_3, K_6, K_7, K_8 and K_9 are discrete absorption components of shell origin but not highly (blue) shifted absorptions (i.e. HVA), noted in the papers by Kaufer et al. (1996b), Israelian et al. (1997). While K_2, K_4 and K_5 are artificially formed components because of the appearance of emission in the absorption core.

During the whole time of observations as it was noted earlier by other authors (Aydin, 1972; Rozendhal, 1973; Inoue, 1979; Kontizas and Kontizas, 1981; Kaufer et al., 1996a; Verdugo et al., 1999) the Hα line had a P Cyg profile. From our observations the enhancement in the emission intensity on the red wing of the Hα line is normally accompanied by the decrease in central intensity of the absorption and vice versa. But on the nights 31.08.98 and 01.09.98 the decrease in the intensity of the emission component is accompanied by the decrease in the absorption component intensity, Table 1 (D–E). This is caused by the appearance of emission at the centre of the absorption core, Fig. 1 (E). As can be seen from Fig. 1 (D), this emission is not observed on the previous nights (27 and 28.08.98). The appearance of this emission is difficult to explain by the shift of one absorption component with respect to another. The differential shifts for the blue and red halves of the absorption contour (at -5.0 and -1.0 km/s, respectively) that we recorded at level IV are insufficient to explain this phenomenon, Table 3 (E–D). On the other hand, on 01.09.98 the intensity of this emission grows by $\Delta r_\lambda \approx 0.014$ as compared with 31.08.98, while the intensities of the absorption components K_5 and K_1 decrease, on the average, by $\Delta r_\lambda \approx 0.007$. But during these two nights neither the absorption itself nor its individual components show radial velocity variations within the measurement errors. Probably we observe the onset of a large-scale ejection of matter from the envelope of the star.

It should be noted that at level IV the amplitude of the absorption radial velocity variation, obtained as difference of the experimental velocity values in Table 2 (for instance at level $r_\lambda = 0.65, 22$ km/s), is considerably lower than 37.5 km/s found from the amplitudes for the blue and red halves of the absorption contour 56 and 19 km/s, respectively. The investigations show that these discrepancies result from the superposition of the absorption and emission components of shell origin. As a result the blue and/or red halves of the absorption contour show additional shifts. In the example presented the additional shifts of the blue and red halves of the absorption contour are 24 and 7 km/s, respectively. So, our method allows us to estimate the share of contribution made by the additional absorption and emission components to the radial velocity variation of the blue and red halves of the absorption contour.

In resolution (≈ 1.5 times as high) and in quality our spectral data compare favourably to the material obtained by the "Heidelberg" group (Kaufer et al., 1996a). As to the number of spectrograms, time resolution and duration of observations, their data are superior to ours. In spite of this our method of studying time variations of the absorption radial velocities permitted us to reveal some features of the Hα profile variability. In contrast to the "Heidelberg" group, we have found that the "basic" absorption itself is variable and the variability is different at different levels of residual intensity. The comparison of radial velocities of the absorption and emission components or their details observed in the blue and red halves of the absorption contour, as distinct from Kaufer et al. (1996a), did not allow us to detect the features of symmetry of these phenomena with respect to the radial velocity of the centre of mass of the star.

5. Conclusions

Thus, our investigations have shown that to reveal the picture and the causes of variability of the Hα line profile in the spectrum of the supergiant α Cyg, a detailed study of the time variation of the absorption radial velocity, blue and red halves of its contour at different levels of residual intensity is necessary. This method makes it possible to determine at different absorption levels: the value of the radial velocity gradient for the blue and red halves of absorption; the share of the contribution made by the blue and red halves of its contour to the absorption radial velocity variation; the contribution of additional absorption and emission components to the variation of the radial velocity of the blue and red halves of the absorption contour.

From the value of the gradient of the radial velocity and from its variation with time the Hα absorption can be divided into four levels. The radial velocity variation of the absorption, blue and red halves of its contour, full width of the absorption differ for different levels. The amplitudes of these variations also differ for these levels, i.e. for different atmosphere layers where these levels effectively form. This points out to stratification of the radial velocity in the upper atmosphere layers where the stellar wind begins to form.

By the character of the radial velocity variation one can separate 5 cases of variability of the "basic" Hα line absorption. Four of them are associated with the variations of the velocity field caused by radial and/or non-radial pulsations existing in the atmosphere of the star, and the fifth is due to the appearance of additional shell details. At some moments of observation absorption and emission components which form in the star envelope as a result of ejection of matter from the surface of the star, which is evidence of the non-stationary, non-spherical stellar wind.

Note that with accumulation of sufficient statistical data our method of investigation of radial velocity variations with time in the upper layers of the atmosphere will give valuable information about the velocity field and its time variation in the upper layers of the atmosphere of the star.

Acknowledgements. The author thanks N.A. Sakhibullin (Kazan University), V.E. Panchuk and E.L. Chentsov (SAO RAS), R.Kh. Salmanzade (ShAO) for valuable advice in the discussion of results and also Kh.M. Mikailov, M.E. Shukurov and I.A. Alekberov for help in observations. The work was supported by the RFBR through grant 02-02-16085.

References

Aydin C., 1972, Astron. Astrophys., **19**, 369
Aufdenberg J.P., Hauschildt P.H., Baron E., et al., 2002, Astrophys. J., **570**, 344
Chentsov E.L., 1995, Astrophys. Space Sci., **232**, 217
Galazutdinov G.A., 1992, Preprint SAO RAS, **92**, Nizhnij Arkhyz
Inoue M.O., 1979, Publ.Astron.Soc.Japan, **31**, 11
Israelian G., Chentsov E. and Musaev F., 1997, Mon. Not. R. Astron. Soc., **290**, 521
Kaufer A., Stahl O., Wolf B., et al., 1996a, Astrophys. J., **305**, 887
Kaufer A., Stahl O., Wolf B., et al., 1996b, Astrophys. J., **314**, 599
Kaufer A., Stahl O., Wolf B., et al., 1997, Astrophys. J., **320**, 273
Kontizas F., Kontizas M., 1981, Astron. Astrophys. Suppl. Ser., **45**, 121
Lucy L.B., 1976, Astrophys. J., **206**, 499
Musaev F.A., 1993, Pis'ma Astron. Zh., **19**, 776
Rzayev A.Kh., Hasanov N.O., Mikailov Kh.M., Alekberov I.A., Shukurov M.E., 1999a, Tsirkular ShAO, **95**, 3
Rzayev A.Kh., Mikailov Kh.M., Alekberov I.A., Shukurov M.E., Guliyev A.S., 1999b, Tsirkular ShAO, **97**, 3
Rozendhal J.D., 1973, Astrophys. J., **182**, 523
Verdugo E., Talavera and Gomez de Castro A.I., 1999, Astron. Astrophys. Suppl. Ser., **137**, 351